Proceedings Paper:
Hong, B, Sun, L, Wang, GP et al. (2020) Millimeter-wave Dual-Function Hollow Metal Waveguide to Microstrip Transition and Bandpass Filter based on ENZ Metamaterial. In: Proceedings of the 2019 Research, Invention, and Innovation Congress (RI2C 2019). 2019 Research, Invention, and Innovation Congress (RI2C 2019), 11-13 Dec 2019, Bangkok, Thailand. IEEE. ISBN: 978-1-7281-4101-5.

https://doi.org/10.1109/RI2C48728.2019.8999915

Millimeter-wave Dual-Function Hollow Metal Waveguide to Microstrip Transition and Bandpass Filter based on ENZ Metamaterial

Binbin Hong, Lei Sun, and Guo Ping Wang
Institute of Microscale Optoelectronics
Shenzhen University
Shenzhen, China
b.hong@szu.edu.cn, lsun@szu.edu.cn, gpwang@szu.edu.cn

Robert Richardson
School of Mechanical Engineering
University of Leeds
Leeds, United Kingdom
r.c.richardson@leeds.ac.uk

Nonchanutt Chudpooti
Industrial Electric and Control System Research Center,
Department of Industrial Physics and Medical Instrumentation,
Faculty of Applied Science,
King Mongkut's University of Technology North Bangkok
Bangkok, Thailand
nonchanutt.c@sci.kmutnb.ac.th

Ian D. Robertson and Nutapong Somjit
School of Electronic and Electrical Engineering
University of Leeds
Leeds, United Kingdom
i.d.robertson@leeds.ac.uk, n.somjit@leeds.ac.uk

***Abstract*—This paper presents a novel design of a millimeter-wave dual-function in-plane hollow metal waveguide to microstrip transition and bandpass filter based on epsilon-near-zero (ENZ) metamaterial. A hollow metallic rectangular waveguide (HMRW) that operates near its cut-off frequency of the fundamental TE_{10} mode is used to mimic the ENZ metamaterial, allowing the wave to tunnel through the waveguide with an effectively infinite phase-velocity. As a waveguide transition, the ENZ waveguide directly interconnects HMRW and microstrip in the same plane with a minimum insertion loss of 0.7 dB at the 33.06 GHz, overcoming the significant impedance mismatch and geometry difference between HMRW and Microstrip. As a bandpass filter, the design has a near-flat passband with the minimum insertion loss of 0.7 dB and a bandwidth of 1.31 GHz centered at 32.96 GHz, which leads to a Q-factor of 25.17. The work offers a step towards a novel dual-function waveguide transition and bandpass filter that can be used in a variety of functional components for millimeter-wave multichip modules and hybrid integrated circuits.**

Keywords—Waveguide transition, bandpass filter, epsilon-near-zero, metamaterial

I. INTRODUCTION（0.7 页）

Materials with unconventional permittivity and permeability have attracted much attention due to their extraordinary electromagnetic properties. Metamaterials which can tailor the permittivity and permeability by using artificial microstructures have created the opportunity for designing new materials with unusual electromagnetic responses [1, 2]. Recently, a class of epsilon-near-zero metamaterials, which possesses near-zero effective refractive index and hence effectively zero phase variation in the medium, has displayed a wealth of exotic phenomena, such as tunneling [3, 4], enormous field enhancement [5], highly directive emission [6], and significant optical nonlinearity [7]. In nature, the ENZ behavior can be found in noble metals [8, 9], plasmas [10], doped semiconductors [11], polar dielectrics [12], transparent conducting oxides [13], etc. To efficiently manipulate the electromagnetic wave, various artificial microstructures have been realized as the ENZ mediums, such as metal-coated waveguides near the cut-off frequency [14 - 17], metallic nanowires array in the dielectric medium [18, 19], and metal-dielectric multilayer structures [20, 21]. Since the plasma frequencies of noble metals are in the ultraviolet region, it is more common to design ENZ metamaterials using metal-dielectric composite structures in the optical domain. For millimeter-wave applications, the metal-coated waveguides that operate near the cut-off frequency of its propagation modes, which displays near-zero effective permittivity ($\varepsilon_{\mathrm{eff}}$) and refractive index ($n_{\mathrm{eff}}$), has been used to mimic those ENZ metamaterials, which is also known as ENZ waveguides [14].

ENZ waveguides have extremely large phase velocities and consequently large guide wavelengths. Since the phase velocity of the ENZ waveguide is much larger than the speed of light, any mediums between the input and output faces of the ENZ waveguide can be physically far but electrically near and will appear to be electrically small compared with the wavelength. Under this condition, the electromagnetic wave tends to tunnel through the ENZ medium following the Fermat's principle. The ENZ waveguides have been used in filters [22 - 26], sensors [27 - 29], coaxial-to-waveguide transition [30], and antenna [31, 32]. So far, rare work been done on the hollow metal waveguide to microstrip transition based on ENZ metamaterial. To interconnect the hollow metal waveguide and microstrip in a compact form is of great interest for millimeter multichip modules and hybrid integrated circuits applications, as different functional components may use different types of host waveguides. Based on the tunneling effect, ENZ waveguide can interconnect the hollow metal waveguide and microstrip efficiently at selected frequency band, in spite of the significant impedance mismatch and geometry difference between these waveguides, making it an interesting alternative waveguide transition method to the other classic schemes using microstrip probe [33 - 35], patch [36, 37], fin line [38, 39], and step matching [40, 41].

This paper presents a Ka-band standard WR-28 hollow metallic rectangular waveguide to 50 Ω microstrip transition

This work was supported in part by the National Natural Science Foundation of China under Grant 11734012 and Grant 11574218 and in part by the Guangdong Natural Science Foundation under Grant 2018A030313939.

using the ENZ waveguide centered at around 33 GHz. The minimum insertion loss is 0.7 dB occurring at 33.06 GHz. In the meantime, the proposed design also acts as a bandpass filter with a bandwidth of 1.31 GHz centered at 32.96 GHz ranging from 32.32 GHz to 33.63 GHz and a Q-factor of 25.17. The center operating frequency can be easily tuned by changing the *H*-plane width of the ENZ waveguide, and the Q-factor can be tuned by adjusting the *E*-plane height and length of the ENZ waveguide. The proposed novel dual-function waveguide transition and bandpass filter may be used in various functional components for millimeter-wave applications.

II. Principle

Firstly, we investigate the ENZ tunneling effect using a classic setup [14] which uses an ENZ narrow waveguide channel to connect two standard WR-28 hollow metallic rectangular waveguides, shown in Fig. 1(a). When the metal wall is set as perfect electric conductor (PEC), no Ohmic loss is induced in the waveguide. The propagation constant for the fundamental TE_{10} mode can be expressed as

$$\beta = \sqrt{(2\pi f/c)^2 - (\pi/w)^2}, \quad (1)$$

where w is the waveguide *H*-plane width, c is the speed of light, and f is the operating frequency. The effective refractive index $n_{\text{eff}} = \beta/k_0$, where k_0 is the free-space wavenumber. The effective relative permittivity for the fundamental TE_{10} mode in an HMRW is defined as [42]

$$\varepsilon_{\text{eff}} = \varepsilon_0(1 - (c/2fw)^2). \quad (2)$$

At the cut-off frequency, $f = c/2w$, $\beta = n_{\text{eff}} = \varepsilon_{\text{eff}} = 0$ which lead to an infinite phase velocity. When the metal wall is treated as a lossy conductor, the propagation constant does not drop to zero below the ideal cut-off frequency due to the presence of surface evanescent wave. To fulfill the condition $Re(\tilde{\varepsilon}_{eff}) = 0$ for a zero-permittivity medium, $n_{\text{eff}} = k_{\text{eff}}$ or equivalently $\alpha = \beta$, where k_{eff} is the effective extinction coefficient and α is the attenuation constant. So, for a lossy waveguide, the zero permittivity happens slightly below the cut-off frequency, instead of at the exact ideal cut-off frequency, allowing $\alpha = \beta$.

In Fig. 1, hollow metallic rectangular waveguides are used in CST MWS simulation, and the cladding metal is set as copper with a fixed conductivity of 5.8×10^7 S/m. Fig. 1(b) shows that effectively tunneling between the HMRWs is archivable and tunneling frequency points are slightly below the ideal cut-off frequencies of the TE_{10} mode of the ENZ waveguide. Here, f_{c1}, f_{c2}, and f_{c3} correspond to the ideal cut-off frequency for w_1, w_2, and w_3, respectively. Fig. 1(c) presents that the Q-factor of the transmission spectrum increases with the decrease of the ENZ waveguide *E*-plane height, at a cost of greater insertion loss. Besides, the tunneling frequency is closer to the ideal cut-off frequency (f_c) when the height is smaller. The dependence of the transmission properties on the length of the ENZ waveguide is studied in Fig. 1(d). The longer the ENZ waveguide is, the higher the Q-factor and the closer the operating frequency to the ideal cut-off frequency are, though the insertion loss also increases with the increase of the ENZ waveguide length. Also, a longer ENZ waveguide brings the high order resonant tunneling mode closer to the fundamental one. In summary, one can effectively tune the operating frequency and Q-factor of the ENZ tunneling behaviors to fulfill the demands, with the insertion losses, fabrication difficulties, and high-order modes distortions being considered as potential tradeoffs.

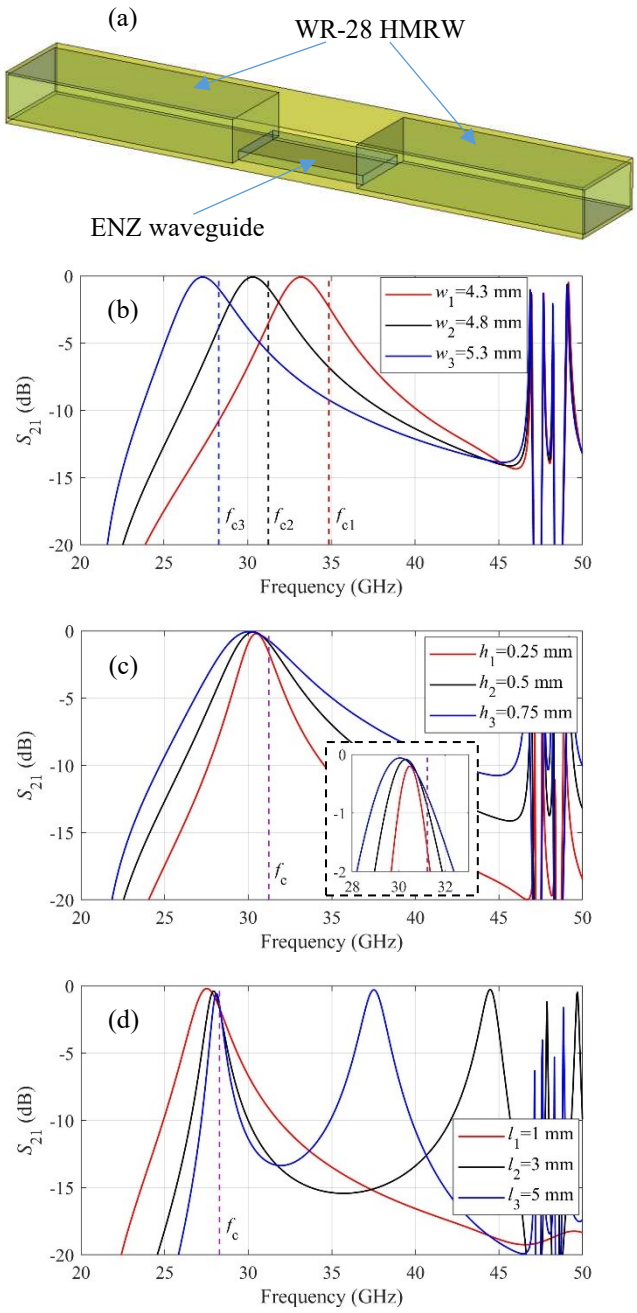

Fig. 1. ENZ waveguide tunning effect. (1) Geometry illustration. Lossy copper is used as the metal walls. (2) Transmission coefficient with different ENZ waveguide *H*-plane width. The *E*-plane height and the length are fixed at 0.5 mm and 1 mm, respectively. The vertical dashed lines indicate the ideal cut-off frequency for the ENZ waveguide corresponding widths. (3) Transmission coefficient with different ENZ waveguide *E*-plane height. The *H*-plane width and the length are fixed at 4.8 mm and 1 mm, respectively. The inset shows the zoomed view around the peaks. (3) Transmission coefficient with different ENZ waveguide length. The width and height are fixed at 5.3 mm and 0.25 mm, respectively.

III. Results

A. An ENZ Waveguide bandpass filter

With single ENZ waveguide, there are only a few limited parameters to tune the transmission properties for the

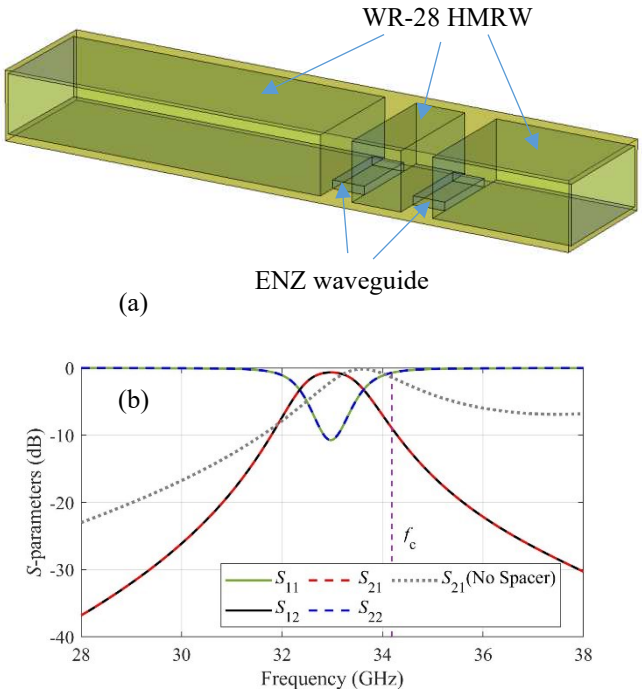

Fig. 2. A modified ENZ waveguide bandpass filter. (a) Geometry illustration. The width, height and length of the two ENZ waveguides are 4.385 mm, 0.508 mm, and 2 mm, respectively. A spacer is introduced in the middle of the ENZ waveguides to increase the Q-factor. (b) The *S*-parameters, including the transmission coefficient for the original design without a spacer for comparison purpose. The vertical dashed line indicates the ideal cut-off frequency for the ENZ waveguide with w=4.385 mm.

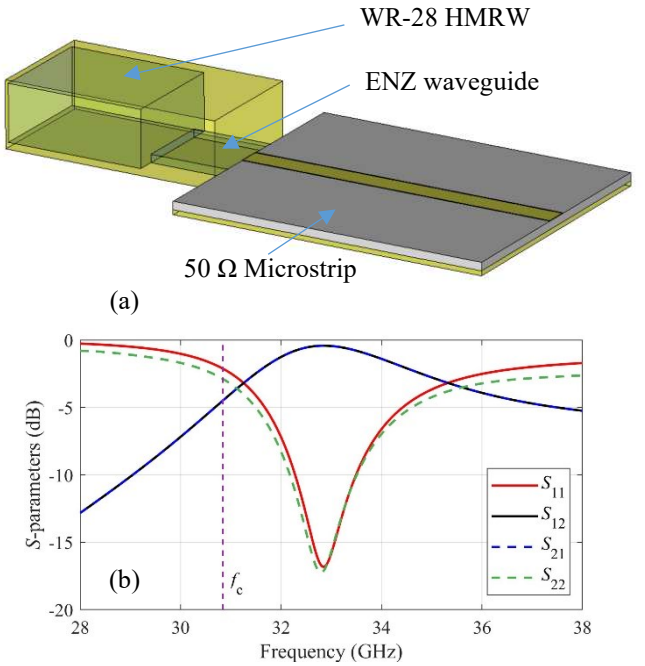

Fig. 3. A hollow metallic rectangular waveguide to microstrip transition. (a) Geometry illustration. The width, height and length of the ENZ waveguide are 4.86 mm, 0.508 mm, and 5 mm, respectively. (b) The *S*-parameters for the HMRW to microstrip transition. The vertical dashed line indicates the ideal cut-off frequency for the ENZ waveguide with w=4.86 mm.

tunneling effect, and it is difficult to fulfill all design goals at the same time, such as low insertion loss and high Q-factor, as well as good high order transmission channel suppression. Fig. 2(a) shows a modified design for an ENZ waveguide bandpass filter. A short section of standard HMRW is put in the middle of two ENZ waveguides as a spacer. Compared with the original design without a spacer, as shown in Fig. 2(b), the Q-factor are increased and the transmission at frequencies other than the selected operating band is significantly suppressed, though the insertion loss at the passband is slightly increased and the operating frequency is also shifted. Interestingly, the spacer does not act as a resonance cavity because it is not shorted at the longitudinal direction due to ENZ tunneling effect and not standing wave is formed in it. It increases the Q-factor by increasing the impedance mismatch for frequencies other than the selected tunneling band.

B. An HMRW to Microstrip Waveguide Transition

Fig. 3(a) shows a waveguide transition between the standard WR-28 HRMW and the 50 Ω microstrip utilizing the tunneling effect of the ENZ waveguide. The microstrip uses standard Rogers RT/Duroid 5880 board. The permittivity and the loss tangent of the dielectric substrate are 2.2 and 0.0009, respectively. The thicknesses for the dielectric substrate and the top signal line are standard 0.508 mm and 0.035 mm, respectively. The width for the signal track is chosen as 1.5 mm making the line impedance for the microstrip near 50 Ω at 33 GHz. The effective permittivity and refractive index of the microstrip are 1.87 and 1.37, respectively.

Efficient transition has been achieved around the tunneling point with the minimum insertion loss of 0.42 dB occurring at 32.85 GHz. The 3 dB bandwidth is 3.85 GHz ranging from 31.32 GHz to 35.17 GHz. It should be noted that the ENZ tunneling frequency point for this case occurs above the cut-off frequency, indicating the average permittivity of overall ENZ channel is positive, which will be explained in the next section. Due to the nature of narrow transmission window of the ENZ waveguide, the HMRW to microstrip transition using single ENZ waveguide channel does not support wideband transmission. On the other hand, one can build a dual-function HMRW to microstrip and bandpass filter based on it. To realize a bandpass filter, it is needed to further improve the Q-factor of the current design.

C. Cascaded Full Structure

To further improve the Q-factor of the waveguide transition leads to a cascaded full design which connects the ENZ waveguide bandpass filter with the above HMRW to microstrip waveguide transition using a shared part of standard WR-28 HMRW, as presented in Fig. 4(a). The stage I refers to the ENZ waveguide bandpass filter discussed in Fig. 2, and the stage II refers to the HMRW to microstrip waveguide transition discussed in Fig. 3. The geometrical parameters and material properties remain the same as the previous designs.

Fig. 4(b) presents the *S*-parameters for the full design, as well as the transmission coefficients for the stage I and the stage II for comparison purpose. As both the stage I and the stage II possesses a transmission window at around 33 GHz, the cascaded full structure also exhibits a 3 dB passband ranging from 32.32 GHz to 33.63 GHz, centered at 32.96 GHz. The Q-factor is calculated to be 25.17. For the stage I and the stage II, the Q-factors are 27.04 and 8.62, respectively. Therefore, the Q-factor of the cascaded full design is slightly lower than that of the stage I and much significantly improved compared to the stage II. As discussed in the section II, one can further increase the Q-factor by increasing the length or reduce the *E*-plane height of the ENZ waveguide at a cost of increasing the insertion loss.

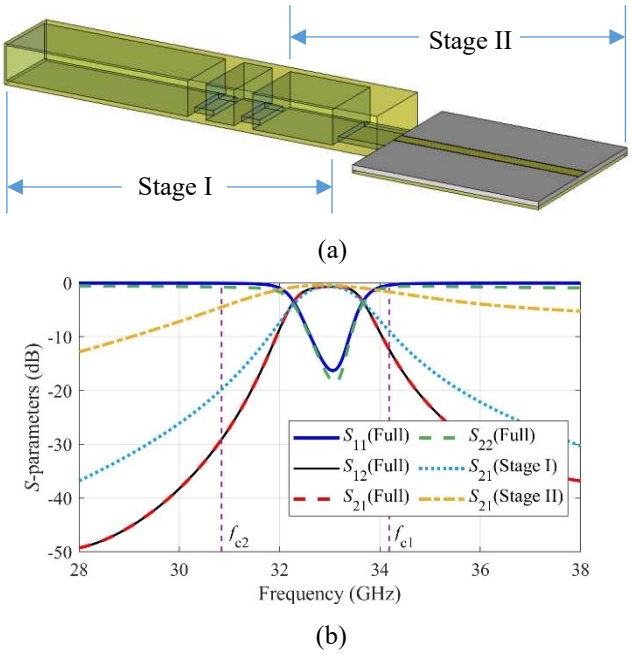

Fig. 4. Cascaded full structure. (a) Geometry illustration. The stage I and the stage II refers to the bandpass filter and waveguide transition shown in Fig. 2(a) and Fig. 3(a), respectively. (b) *S*-parameters for the cascaded full structure, as well as the S_{21} for the stage I and the stage II. The right and left vertical dashed purple lines indicate the ideal cut-off frequencies for the ENZ waveguide in the stage I and stage II, respectively.

Alternatively, one can add a microstrip bandpass filter to the end of the stage II to increase the overall Q-factor.

The minimum insertion loss of the cascaded full structure is 0.7 dB at 33.06 GHz. The electric field pattern and the phase variation along the cascaded full structure at 33.06 GHz are shown in Fig. 5. The fundamental TE_{10} mode in the standard WR-28 HMRW is observed to successfully transfer to the quasi-TEM mode in the microstrip through the ENZ waveguide channels.

Fig. 5(b) presents the phase pattern along with the cascaded full structure, and Fig. 5(c) plots the phase variation along the dashed black line shown in Fig. 5(b). It can be seen that the phase variation in the ENZ channels I and II are near flat indicating a very large phase velocity and thus near-zero permittivity behaviors. While in the ENZ channel III, the phase variation is small initially which corresponds to the rise of the ENZ tunneling phenomenon, but the phase velocity decreases significantly at the end of the ENZ channel to match the phase velocity of the quasi-TEM mode in the microstrip which is close to the speed-of-light in the effective dielectric medium. In other words, the effective permittivity is near zero at the front end of the ENZ channel III and is close to the effective permittivity of the microstrip (1.87) at the back end, so the average effective refractive index is between these two values, which also explains why the tunneling frequency point is above the ideal cut-off of the ENZ waveguide as discussed in the Fig. 3. Since a certain distance is needed for the ENZ channel III so the phase velocity has enough time to change from the extremely large in the ENZ waveguide to the speed of light in the effective medium of the microstrip, if the length of the ENZ channel III is too short, the tunneling effect does not happen, while if the length is too long, the performance will decrease due to the increase of the insertion loss.

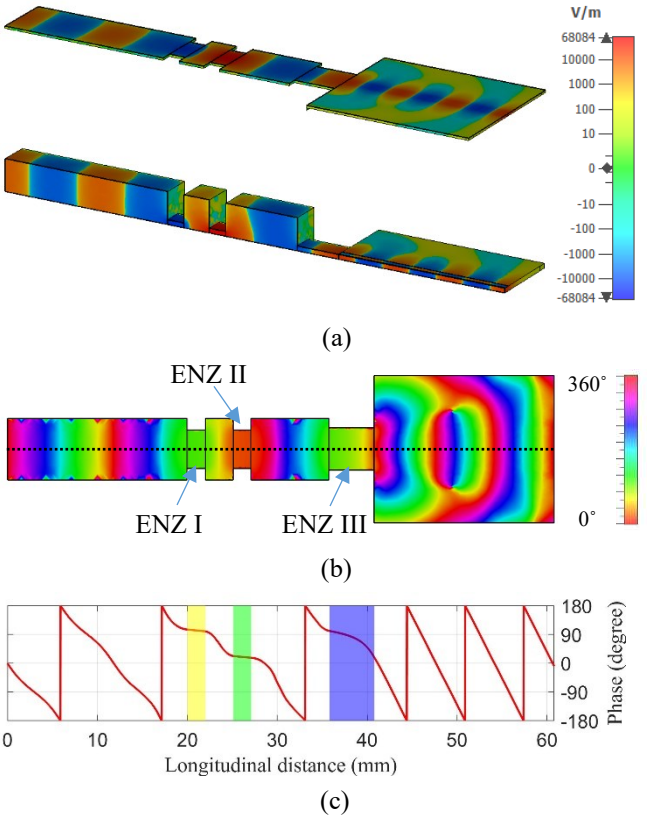

Fig. 5. Wave propagation along with the cascaded full structure. (a) Cut-away views of the y-component of the electric field. (b) Phase pattern in the structure. (c) Phase variation along the dotted black line in (b). The light yellow, green and blue regions correspond to the ENZ I, II and III sections, respectively.

IV. Conclusion

This work presents a novel design of a dual-function HMRW to microstrip transition and bandpass filter at Ka-band using ENZ metamaterials. Efficient transmission is achieved with a minimum insertion loss of 0.7 dB at 33.06 GHz. The bandwidth of the passband is 1.31 GHz centered at 32.96 GHz, and the Q-factor is 25.17. One can adjust the Q-factor to fulfill the demands by changing the width, height, and length of the ENZ waveguide. This work offers a new alternative for the hollow metal waveguide to microstrip transition and is useful for various functional components for millimeter-wave applications.

References

[1] V. G. Veselago, "The electrodynamics of substances with simultaneously negative values of ε and μ", Soviet Phys. Uspekhi, vol. 10, no. 4, pp. 509-514, Jan. 1968.

[2] D. R. Smith, J. B. Pendry, and M. C. Wiltshire, "Metamaterials and negative refractive index", Science, vol. 305, no. 5685, pp. 788-792, 2004.

[3] M. Silveirinha, and N. Engheta, "Tunneling of electromagnetic energy through subwavelength channels and bends using ε-near-zero materials." Physical Review Letters, vol. 97, no. 15, pp. 157403, 2006.

[4] M. G. Silveirinha, and N. Engheta. "Theory of supercoupling, squeezing wave energy, and field confinement in narrow channels and tight bends using ε near-zero metamaterials." Physical Review B, vol. 76, no. 24, pp. 245109, 2007.

[5] N. M. Litchinitser, A. I. Maimistov, I. R. Gabitov, R. Z. Sagdeev, and V. M. Shalaev, "Metamaterials: electromagnetic enhancement at zero-index transition", Optics Letters, vol. 33, no. 20, pp. 2350-2352, 2008.

[6] A. Ourir, A. Redha, and J. de Rosny, "Planar metamaterial based on hybridization for directive emission", Optics Express, vol. 20, no. 16, pp. 17545-17551, 2012.

[7] O. Reshef, I. De Leon, M. Z. Alam, and R. W. Boyd, "Nonlinear optical effects in epsilon-near-zero media", Nature Reviews Materials, vol. 4, pp. 535-551, Aug. 2019.

[8] H. Y. Li, S. M. Zhou, J. Li, Y. L. Chen, S. Y. Wang, Z. C. Shen, L. Y. Chen, H. Liu, and X. X. Zhang, "Analysis of the Drude model in metallic films", Applied Optics, vol. 40, no. 34, pp. 6307-6311, 2001.

[9] P. G. Etchegoin, E. C. Le Ru, and M. Meyer, "An analytic model for the optical properties of gold", The Journal of Chemical Physics, vol. 125, no.16, pp. 164705, 2006.

[10] F. F. Chen, Introduction to plasma physics and controlled fusion, vol. 1, New York: Plenum press, 1984.

[11] N. Kinsey, C. DeVault, J. Kim, M. Ferrera, V. M. Shalaev, and A. Boltasseva, "Epsilon-near-zero Al-doped ZnO for ultrafast switching at telecom wavelengths", Optica, vol. 2, no. 7, pp. 616-622, 2015.

[12] M. G. Silveirinha, and N. Engheta, "Transporting an image through a subwavelength hole", Physical Review Letters, vol. 102, no. 10, pp.103902, 2009.

[13] G. V. Naik, J. Kim, and A. Boltasseva, "Oxides and nitrides as alternative plasmonic materials in the optical range", Optical Materials Express, vol. 1, no. 6, pp. 1090-1099, 2011.

[14] B. Edwards, A. Alù, M. E. Young, M. Silveirinha, and N. Engheta, "Experimental verification of epsilon-near-zero metamaterial coupling and energy squeezing using a microwave waveguide", Physical Review Lletters, vol. 100, no. 3, pp.033903, 2008.

[15] A. Alù, and N. Engheta, "Boosting molecular fluorescence with a plasmonic nanolauncher", Physical Review Letters, vol. 103, no. 4, pp.043902, 2009.

[16] E. J. R. Vesseur, T. Coenen, H. Caglayan, N. Engheta, and A. Polman, "Experimental verification of n= 0 structures for visible light. Physical review letters", vol. 110, no. 1, pp.013902, 2013.

[17] Y. He, Y. Li, Z. Zhou, H. Li, Y. Hou, S. Liao, and P. Chen, "Wideband Epsilon-Near-Zero Supercoupling Control through Substrate-Integrated Impedance Surface", Advanced Theory and Simulations, vol. 2, no. 8, pp. 1900059, 2019.

[18] R. J. Pollard, A. Murphy, W. R. Hendren, P. R. Evans, R. Atkinson, G. A. Wurtz, A. V. Zayats, and V. A. Podolskiy, "Optical nonlocalities and additional waves in epsilon-near-zero metamaterials", Physical Review Letters, vol. 102, no. 12, pp.127405, 2009.

[19] L. V. Alekseyev, E. E. Narimanov, T. Tumkur, H. Li, Y. A. Barnakov, and M. A. Noginov, "Uniaxial epsilon-near-zero metamaterial for angular filtering and polarization control", Applied Physics Letters, vol. 97, no. 13, pp.131107, 2010.

[20] J. Gao, L. Sun, H. Deng, C. J. Mathai, S. Gangopadhyay, and X. Yang, "Experimental realization of epsilon-near-zero metamaterial slabs with metal-dielectric multilayers", Applied Physics Letters, vol. 103, no. 5, pp.051111, 2013.

[21] R. Maas, J. Parsons, N. Engheta, and A. Polman, "Experimental realization of an epsilon-near-zero metamaterial at visible wavelengths", Nature Photonics, vol. 7, no. 11, pp.907, 2013.

[22] D. V. B. Murthy, A. Corona-Chavez, and J. L. Olvera Cervantes, "A novel epsilon near zero (ENZ) tunneling circuit using microstrip technology for high integrability applications", Progress In Electromagnetics Research, vol. 15, pp.65-74, 2010.

[23] N. Vojnovic, B. Jokanovic, M. Radovanovic, F. Medina, and F. Mesa, "Modeling of Nonresonant Longitudinal and Inclined Slots for Resonance Tuning in ENZ Waveguide Structures," IEEE Transactions on Antennas and Propagation, vol. 63, no. 11, pp. 5107–5113, Nov. 2015.

[24] M. Radovanovic and B. Jokanovic, "Dual-Band Filter Inspired by ENZ Waveguide," IEEE Microwave and Wireless Components Letters, vol. 27, no. 6, pp. 554–556, Jun. 2017.

[25] N. Vojnovic, B. Jokanovic, M. Radovanovic, and F. Mesa, "Tunable second-order bandpass filter based on dual ENZ waveguide," in 2015 9th International Congress on Advanced Electromagnetic Materials in Microwaves and Optics (METAMATERIALS), 2015, pp. 316–318.

[26] A. Corona-Chavez, D. V. B. Murthy, and J. L. Olvera-Cervantes, "Novel microwave filters based on epsilon near zero waveguide tunnels", Microwave and Optical Technology Letters, vol. 53, no. 8, pp. 1706-1710, 2011.

[27] V. Pacheco-Peña, M. Beruete, P. Rodríguez-Ulibarri, and N. Engheta, "On the performance of an ENZ-based sensor using transmission line theory and effective medium approach", New Journal of Physics, vol. 21, no. 4, pp.043056, 2019.

[28] H. Lobato-Morales, D. V. B. Murthy, A. Corona-Chávez, J. L. Olvera-Cervantes, J. Martínez-Brito, and L. G. Guerrero-Ojeda, "Permittivity measurements at microwave frequencies using epsilon-near-zero (ENZ) tunnel structure", IEEE transactions on microwave theory and techniques, vol. 59, no. 7, pp.1863-1868, 2011.

[29] Y. Wang, Z. Sun, and P. Xu, "Manipulating the transmission through valve structure composed of zero-index metamaterial", Journal of Physics D: Applied Physics, vol. 50, no. 46, pp.465104, 2017.

[30] A. Alu, and N. Engheta, "Coaxial-to-Waveguide Matching With ε-Near-Zero Ultranarrow Channels and Bends", IEEE Transactions on Antennas and Propagation, vol. 58, no. 2, pp. 328-339, 2009.

[31] J. Kim, A. Dutta, G. V. Naik, A. J. Giles, F. J. Bezares, C. T. Ellis, J. G. Tischler et al, "Role of epsilon-near-zero substrates in the optical response of plasmonic antennas", Optica, vol. 3, no. 3, pp. 339-346, 2016.

[32] D. M. George, C. C. H. Ng Aanandan Chandroth, and P. R. Young. "High-gain narrow-band slotted antenna based on ENZ SIW structure", Journal of Physics D: Applied Physics, vol. 51, no. 13, pp. 135102, 2018.

[33] Y. Leong, and S. Weinreb, "Full band waveguide-to-microstrip probe transitions", In 1999 IEEE MTT-S International Microwave Symposium Digest (Cat. No. 99CH36282), vol. 4, pp. 1435-1438. IEEE, 1999.

[34] Y-C. Shih, T-N. Ton, and Long Q. Bui, "Waveguide-to-microstrip transitions for millimeter-wave applications", In 1988 IEEE MTT-S International Microwave Symposium Digest, pp. 473-475, IEEE, 1988.

[35] Y. Leong, and S. Weinreb, "Full band waveguide-to-microstrip probe transitions", In 1999 IEEE MTT-S International Microwave Symposium Digest (Cat. No. 99CH36282), vol. 4, pp. 1435-1438. IEEE, 1999.

[36] H. Iizuka, S. Kunio, and N. Kikuma, "Millimeter-wave transition from waveguide to two microstrip lines using rectangular patch element", IEEE transactions on microwave theory and techniques, vol. 55, no. 5, pp. 899-905, 2007.

[37] E. Topak, H. Jürgen, and T. Zwick, "Compact topside millimeter-wave waveguide-to-microstrip transitions", IEEE Microwave and Wireless Components Letters, vol. 23, no. 12, pp. 641-643, 2013.

[38] A. Mozharovskiy, A. Artemenko, V. Ssorin, R. Maslennikov, and A. Sevastyanov, "Wideband tapered antipodal fin-line waveguide-to-microstrip transition for E-band applications", In 2013 European Microwave Conference, pp. 1187-1190, IEEE, 2013.

[39] S. Jing, F. Liang, L. Han, and X. Sun, "Waveguide-to-microstrip antipodal finline transition at W band", In 2013 Third International Conference on Instrumentation, Measurement, Computer, Communication and Control, pp. 510-513, IEEE, 2013.

[40] Y. Zhang, A. R. Jorge, A. Z. Kawthar, and J. P. Andrew, "A waveguide to microstrip inline transition with very simple modular assembly", IEEE Microwave and Wireless Components Letters, vol. 20, no. 9, pp. 480-482, 2010.

[41] M. Simone, A. Fanti, G. Valente, G. Montisci, R. Ghiani, and G. Mazzarella, "A Compact In-Line Waveguide-to-Microstrip Transition in the Q-Band for Radio Astronomy Applications", Electronics, vol. 7, no. 2, pp. 24, 2018.

[42] W. Rotman, "Plasma simulation by artificial dielectrics and parallel-plate media", IRE Transactions on Antennas and Propagation, vol. 10, no. 1, pp. 82-95, 1962.